

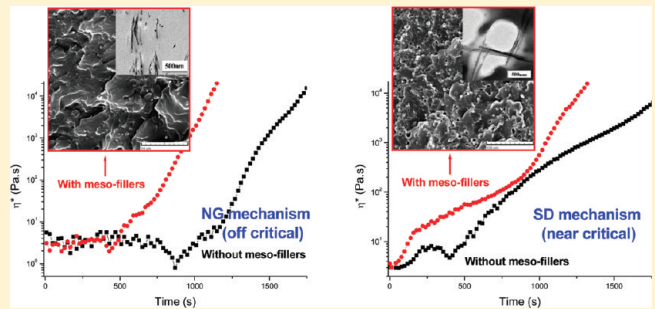
Effect of Mesoscopic Fillers on the Polymerization Induced Viscoelastic Phase Separation at Near- and Off-Critical Compositions

Yi Liu,[†] Xinhui Zhong,[†] Guozhu Zhan,[†] Yingfeng Yu,^{*,†} and Jianyong Jin[‡]

[†]State Key Laboratory of Molecular Engineering of Polymers, Department of Macromolecular Science, Fudan University, Shanghai, 200433, China

[‡]Polymer Innovations Laboratory, School of Chemical Sciences, The University of Auckland, Private Bag 92019, Auckland 1142, New Zealand

ABSTRACT: We have investigated the effect of mesoscopic fillers on the polymerization induced viscoelastic phase separation of thermoplastic modified thermosets at near- and off-critical concentrations using optical microscopy, time-resolved light scattering, dynamic mechanical analyses, and rheological instrument. Mesoscopic fillers including sepiolite and nanosized silica showed a significant enhancement effect in viscoelastic phase separation, and resulted in pronounced differences in the phase structures at all concentrations of polyetherimide modified epoxy resins with dynamic asymmetry. For blends near critical concentration, the introduction of fillers led to much finer phase structure with smaller characteristic length scale. At off-critical composition (i.e., blends with low concentration of slow dynamic component), the strong polymer chain entanglement resulted in enwrapped mesoscopic fillers within a slow dynamic phase. The rheological behavior of the blends clearly demonstrated the significant enhancement effect of mesoscopic fillers in the viscoelastic phase separation. The apparent activation energy of polymer chain mobility obtained from dynamic mechanical study of glass transition reflected strong wrapping behavior of polymer chains on mesoscopic fillers, which were consistent with the rheological and light scattering study.



1. INTRODUCTION

Composite materials containing polymers and fillers are of considerable interests for fundamental scientific study because of their great potential in structural, electrical, and biological applications.^{1,2} In the current polymer binary blend phase separation theories, two major kinds of decomposition mechanisms (spinodal decomposition (SD) and nucleation and growth (NG)) depending on the initial volume fraction located near- or off-critical compositions are studied theoretically based on the solid model or fluid model.³ The phase separation kinetics has been classified into three types: bicontinuous and droplet spinodal decomposition (SD) in the unstable region and nucleation growth (NG) type phase separation in the metastable region.

The early stage of SD and NG phase separation is well described by the Cahn linear theory⁴ and the Lifshitz–Slyozov–Wagner theory,^{5,6} respectively, while the late stage of phase separation follows the self-similar growth and scaling laws.⁷ In both the diffusion controlled solid model and the hydrodynamic transport controlled fluid model, interfacial tension plays a critical role during the phase separation process. However, all of the above theories are based on the concept of dynamic universality, which exhibits fundamental differences to polymer blends with unique contrast of viscoelasticity.⁸

For complex fluids like polymer solutions and colloidal suspensions, etc., Tanaka et al.⁹ found a quite unusual phase

separation, named “viscoelastic phase separation”, which exhibited intrinsic “dynamic asymmetry” due to large differences either in size or in glass transition temperature between their components under deep-quench conditions. For compositions far away from critical concentration via NG or droplet SD mechanism, “moving droplet phase” like elastic gel balls showed long-term dynamic stability rather than thermodynamic stability due to the viscoelastic property of polymers.¹⁰ While at near-critical composition via SD mechanism, a network-like structure dominated by the elastic force-balance condition was formed initially, and then relaxed to a round shaped structure by the interface tension provided there was sufficient phase separation time.⁹

Apart from the influence of polymeric viscoelasticity on phase separation, polymer blends/filler composite systems also exhibited large differences from the traditional dynamic symmetric binary blends. Fillers with size in micrometers were initially studied and showed preferential immersion to one of the phases. The phase structures depended on surface affinity and mobility of the particles.¹¹ Furthermore, the effects of nanoscale fillers on the phase separation behavior of binary polymer blends or block copolymers had also been widely

Received: November 3, 2011

Revised: March 2, 2012

Published: March 5, 2012

studied both by experimental observation^{12–15} and by theoretical simulation^{16–19} in recent years. In binary blends containing spherical nanofillers, the fillers can only slightly affect the phase separation behavior if they interact more attractively with one particular polymer.²⁰ Even so, with well controlled processing conditions such as dispersing nanofillers into surface unfavorable polymer at first, nanofillers may act as compatibilizing agents of immiscible polymer blends,^{21,22} where nanofillers were locked at the interfaces between the immiscible fluids and generate longstanding metastable phase structure.^{23,24}

While most of the literature work focused either on the thermodynamic effect of nanoparticles with dimensions lower or comparable to polymer chain size or on the surface affinity of fillers on the kinetics of phase separation process, to our best knowledge, the effect of mesoscopic fillers on the viscoelastic properties of phase separation in polymer blends has not been studied yet, especially with dynamic asymmetry.

Recently, we have reported a significant enhancement effect of meso-filters in viscoelastic phase separation of dynamic asymmetric polymer blends.²⁵ Due to the entanglement from polymer chains, meso-filters of different shapes are preferentially immersed into the slow dynamic phase, which further increases the dynamic asymmetry and enforces elastic-force balance condition in phase separation. In the case of sufficiently high volume fraction and good dispersion, mesoscopic fillers conducted to pronounced slowing down of the phase separation process, and resulted in refined structures with sharply decreased characteristic length scale.

Our previous work focused on the effect of the shape and size of meso-filters on the viscoelastic phase separation at critical composition. As a continuation of our earlier work,²⁵ in this article, we studied the effect of meso-filters on the morphology and the stress coupling of dynamic asymmetric polymer blend at near- and off-critical composition. We demonstrated the “enhanced viscoelastic effect” of meso-filters in the polymerization induced viscoelastic phase separation in both near- and off-critical composition via SD or NG mechanisms. Preferential distribution of meso-filters in slow dynamic phases due to chain entanglement dominated the viscoelastic phase separation at earlier stages, and thus caused distinct differences of phase structure compared with blends without fillers.

2. EXPERIMENTAL SECTION

2.1. Materials. The epoxy oligomer used, JEH-012, was provided by Changshu Jiafa Chemical Co. (Jangsu, China) and is a modified low viscosity liquid tetraglycidyl-4,4'-diaminodiphenylmethane epoxy resin (TGDDM) with an epoxy equivalent of 115–125 g equiv⁻¹. The curing agent 4,4'-diamino-diphenylsulfone (DDS) was provided by the Sino-pharm Chemical Reagent Co. (Shanghai, China). The commercial thermoplastic polyetherimide, Ultem 1000, polymerized from 2,2'-bis[4-(3,4-dicarboxyphenoxy)phenyl]-propane dianhydride (BisA-DA) and *m*-phenylenediamine was provided by General Electric with a reported weight-average molecular weight of 3.0×10^4 and polydispersity of about 2.5.

Sepiolite, the rod-like mesoscopic inorganic filler with approximately 20 nm in diameter and several micrometers in length, was provided by Tolsa (Spain). To ensure good dispersion in polymer blends, sepiolite was surface modified with the silane coupling agent 2,3-epoxy propoxy propyltrim-

thoxysilicane according to the procedure used by the literature.²⁶

2.2. Specimen Preparation. The compositions of the formulations are collected in Table 1. The formulations contain 0 or 2 wt % of fillers and 0, 5, and 13 wt % of thermoplastics (PEI).

Table 1. Name and Composition of the Samples Studied (Filler, Thermoplastics, Epoxy, and DDS) for the Different Formulations

sample	sepiolite	PEI	TGDDM	DDS
neat epoxy			66	34
Ep-Sep2	2		64.7	33.3
PEI-5		5	62.7	32.3
PEI-13		13	57.4	29.6
PEI-5 Sep2	2	5	61.4	31.6
PEI-13 Sep2	2	13	56.1	28.9

Fillers were added to the epoxy oligomer under nitrogen atmosphere with vigorous stirring and ultrasonication at 100 °C for 6 h, and a homogeneous epoxy/fillers mixture was obtained. Thermoplastics PEI was dissolved in methylene chloride (CH_2Cl_2) and mixed with epoxy at room temperature. After most of the solvent was evaporated at 60 °C, the epoxy–thermoplastic blends were put under a vacuum at 120 °C for 2 h to remove the residual solvent. Then, a stoichiometric amount of curing agent DDS was dissolved in the epoxy mixture with stirring at 150 °C until the mixture was homogeneous. The samples were degassed under a vacuum for another few minutes and then cooled to –10 °C to prevent further curing. For thermal and mechanical testing, bar samples were cured following the procedure: 150 °C/4 h, 180 °C/2 h, and 200 °C/4 h.

2.3. Experimental Techniques. A PerkinElmer Pyris 1 DSC instrument was used for the study of the curing reaction. The isothermal curing conversion was calculated from residual exotherms observed in scans in the temperature range 50–350 °C, with heating rates of 10 °C/min and normalized by the total exotherms for uncured samples.

The phase-separation process during the isothermal curing reaction was observed at real time and *in situ* on the self-made time-resolved light scattering (TRLS) instrument with controllable hot chamber.^{27,28} The change of the light scattering profiles was recorded at appropriate time intervals during isothermal curing. The blend of epoxy monomer with thermoplastics for TRLS observation was prepared by melt-pressing the film.

Optical light microscopy (OM) experiments were performed with an Olympus BX51P microscope equipped with an Instec HCS410 hot stage.

Transmission electronic microscopy (TEM) was performed with a JEM-1200EX TEM; ultrathin films of cured blends for TEM observation were prepared with an ultramicrotome (Leica Ultracut R) equipped with a diamond knife.

The morphologies of the isothermally cured blends were observed under a scanning electron microscope (SEM, Tescan TS 5163MM) for samples fractured in liquid nitrogen. All samples were coated with gold and mounted on copper mounts.

The melt viscosity variations of the blends during cure reaction were recorded on an Ares-9A rheometry instrument: about 1 g of the blend was sandwiched between two round

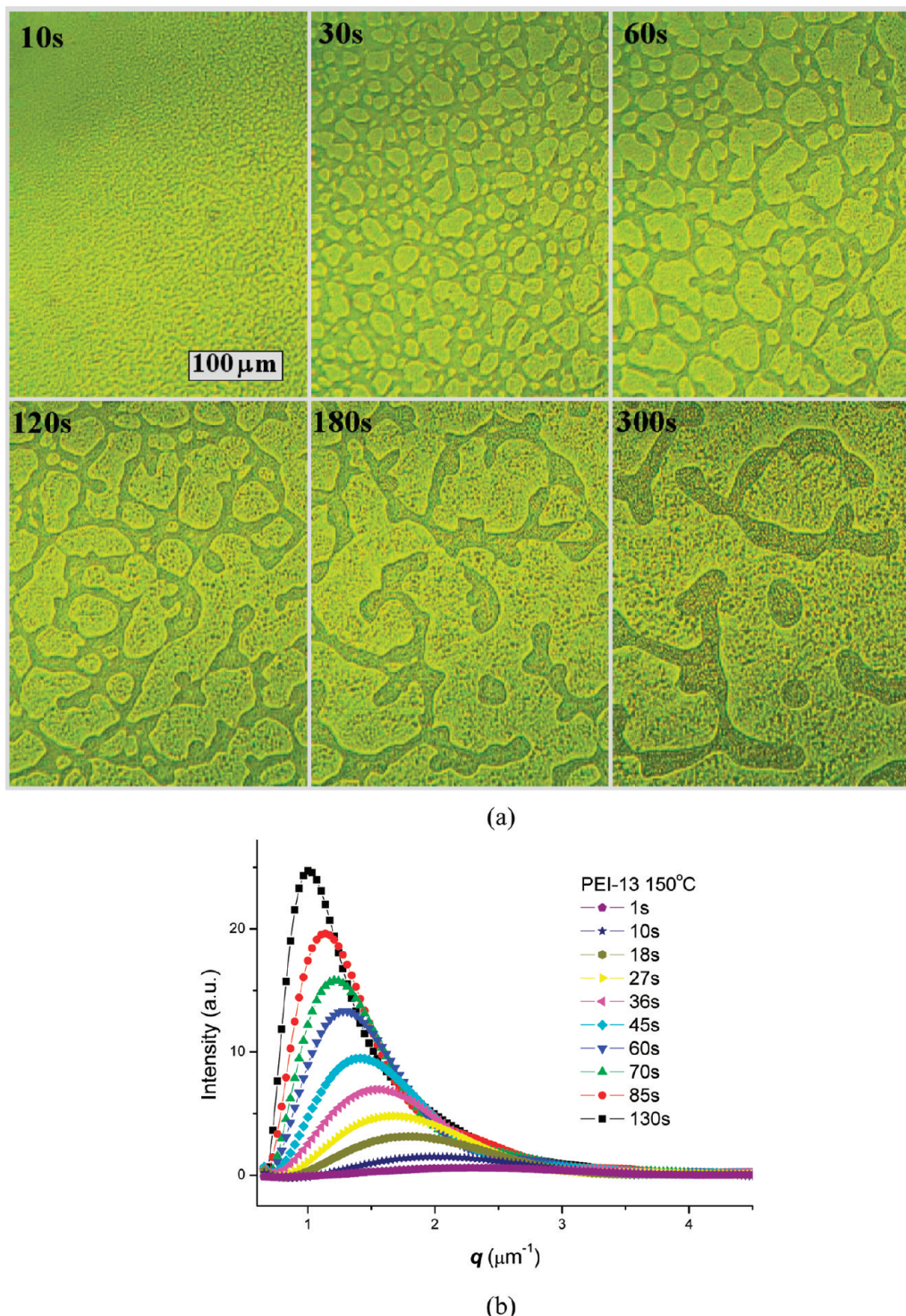


Figure 1. Phase structure evolution of PEI-13 observed by OM and TRLS cured at 150 °C: (a) morphology observed by OM; (b) TRLS study of scattering vector versus phase separation time.

fixtures and softened at 60 °C for 2 min. The plate distance was then adjusted to about 1.5 mm, and the temperature was raised quickly at a rate of 100 deg/min to the preset curing temperature. All the blends were tested under a parallel plate mode with a controlled strain of 1% and test frequency of 1 Hz.

The dynamic mechanical properties were collected with a Netzsch DMA 242 operating in the three-point-bending mode at multi-oscillation frequencies of 1, 2, 5, and 10 Hz. The specimens for DMA were prepared in the form of bars with a

nominal dimension of 1 × 15 × 50 mm³, and the data were collected from ambient temperature to 260 °C at a scanning rate of 3 °C/min.

The Izod impact test was performed at room temperature by means of an Izod 5110 impact tester, according to ISO 180-2000 using unnotched rectangular specimen testing. The pendulum employed had a kinetic energy of 1 J. The impact strength was obtained by taking the average values of 10 specimens.

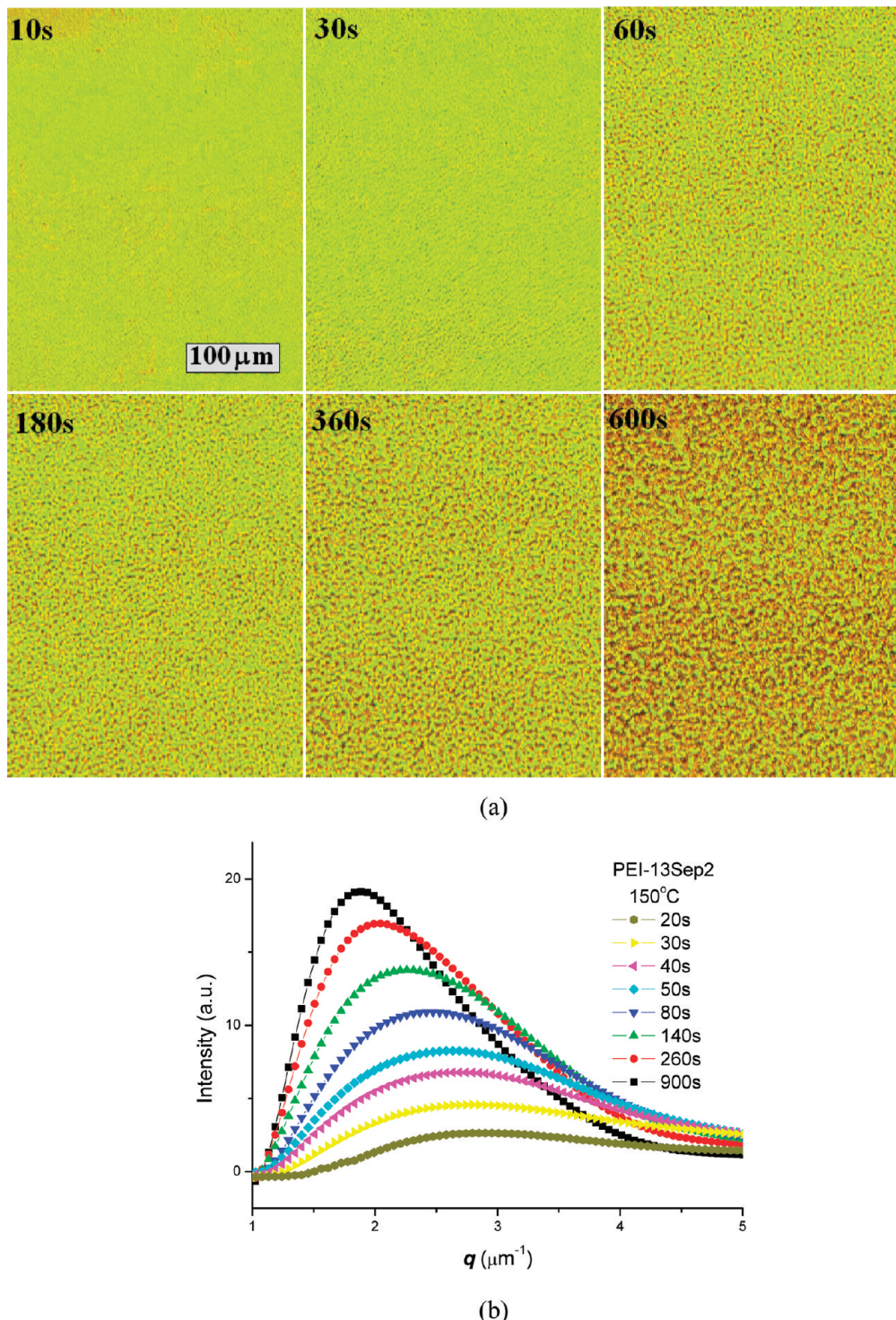


Figure 2. Phase structure evolution of PEI-13Sep2 observed by OM and TRLS cured at 150 °C: (a) morphology observed by OM; (b) TRLS study of scattering vector versus phase separation time.

3. RESULTS AND DISCUSSION

3.1. Effect of meso-Fillers in Blends at Near-Critical Composition.

Polymerization induced viscoelastic phase separation (PIVPS) has been studied recently in various systems of thermoplastic modified thermosetting resins.^{27–34} On the basis of our earlier findings on the enhancement effect of meso-filler in the PIVPS of polyethersulfone modified diglycidyl ether of bisphenol A (DGEBA) epoxy systems,²⁵ we further expanded our study of this meso-filler enhanced effect

in various blends with dynamic asymmetry during the PIVPS process.

Figure 1 shows a typical evolution process of the PIVPS in the PEI-TGDDM system (sample PES10) studied by OM and TRLS; similar results have been observed in numerous works.^{27–34} At the beginning of the phase separation via SD mechanism ($t = 10$ s), a microbicontinuous phase structure was observed by OM as is always found in ordinary phase separations. As the polymerization proceeds ($t = 30$ s), the

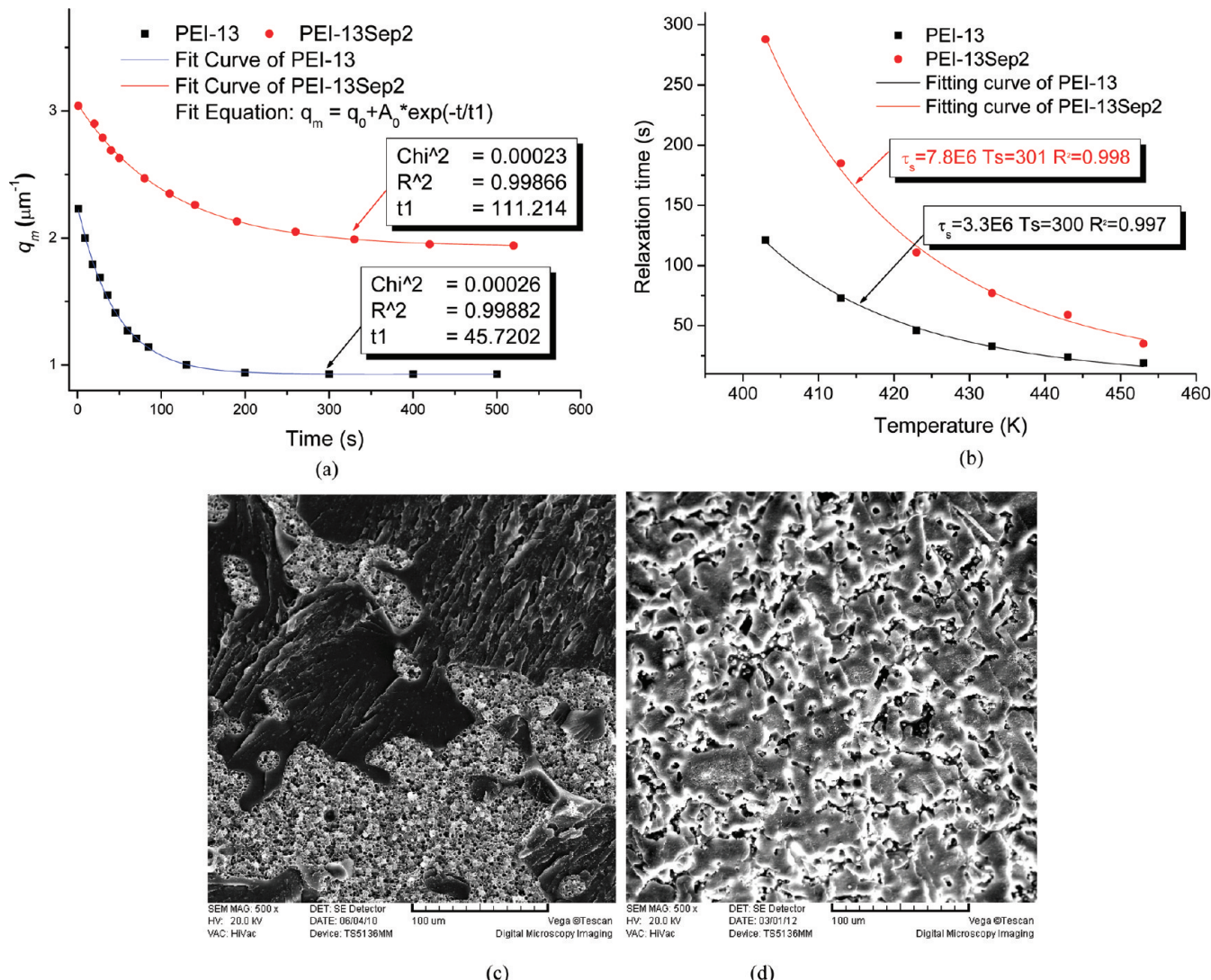


Figure 3. Relaxation time versus temperature and phase structure of PEI-13 and PEI-13Sep2. (a) q_m versus time at 150 °C. The points correspond to the experiment data, and the line corresponds to the result simulated by $q_m(t) = q_0 + A_1 e^{-t/\tau}$. (b) Plots of the relaxation time versus temperature. The points correspond to experimental data, and the line corresponds to results simulated by the WLF equation. (c) Morphology of PEI-13 observed by SEM. (d) Morphology of PEI-13Sep2 (etched by chloroform) observed by SEM.

epoxy-DDS precursors diffuse out from the PEI-rich phase (fuscous region) and coarsen rapidly. Then, the morphology size grows quickly with the coarsening of epoxy-rich (light region) of anisotropic shapes ($t = 60$ and 90 s). With the elastic elongation and breaking of the PEI-rich regions, irregular PEI-rich macro-phase domains dispersed in the epoxy-rich matrix are formed ($t = 180$ and 300 s).

Light scattering results (Figure 1b) show a relaxation behavior of phase size (scattering vector), which had been demonstrated to be resulted from the viscoelastic behavior of polymer chains.^{27,28,30,31} Due to the presence of dynamic asymmetry between thermoplastics and thermoset precursors, which was induced by the large differences in molecular mobility, molecular weight, and glass transition temperature of the two components, the viscoelasticity of the slower dynamic phase (thermoplastic-rich phase) increased with the discharging of the thermoset precursor from the thermoplastic-rich phase and eventually behaved as an elastic body. Meanwhile, the less viscoelastic phase (thermoset-rich phase) started to coarsen with time, and the elastic force balance dominated the

morphology instead of the interface tension, which led to the anisotropic shape of the domain.

With the addition of meso-filters in the thermoplastic–epoxy blends (PEI-13Sep2), dramatic change was observed in the evolution process and phase structure (Figure 2). At the early stage of the phase separation, a microbicontinuous phase structure was observed, which was similar to what has been observed in PEI-13. However, rather than coarsening rapidly in the PEI-13, the PEI-rich and epoxy-rich phases in PEI-13Sep2 grow slowly until the chemical gelation of the epoxy. Bicontinuous networks with much smaller characteristic length scales were obtained at the end of phase separation.

Quite different from the sample control, the bicontinuous structure in samples with sepiolite formed at the early stage coarsens slowly to give the network formed by the PEI-rich phase. TRLS showed a much larger scattering vector q_m of PEI-13Sep2 (Figure 2b) than that of the sample without fillers (PEI-13 in Figure 1b). For samples with meso-filters, the initial q_m value was near 3.5 and ends at about 2.0, while samples

without meso-filters had a much smaller \mathbf{q}_m value in the range of ca. 2.0 to 1.

Previous and recent works showed that the evolution of \mathbf{q}_m corresponds to thermosetting precursor droplets and follows a Maxwell-type relaxation equation (eq 1).

$$q_m(t) = q_0 + A_1 e^{-t/\tau} \quad (1)$$

where $\mathbf{q}_m(t)$ is the scattering vector at time t , \mathbf{q}_0 is the initial value at the beginning of phase separation, and τ is the characteristic relaxation time. The time-dependent \mathbf{q}_m from both samples (PEI13 and PEI-13Sep2) fits the Maxwell-type relaxation equation very well (Figure 3a). Table 2 showed the

Table 2. Relaxation Time of PES13 and PES13Sep2 Curing at Different Temperatures

temperature (K)	403	413	423	433	443	453
PEI13 (s)	121	73	46	33	24	19
PEI13Sep2 (s)	288	185	111	96	77	59

same trend at all temperatures; i.e., the relaxation time of the thermoplastic slows down significantly when sepiolite is introduced. Similar light scattering profiles are obtained at all temperatures for the samples. In other words, the much larger relaxation time of the system with meso-filters (PEI-13Sep2) definitely indicated a significant slowdown of phase separation (chain mobility) due to the enhanced viscoelastic effect of meso-filters.

The temperature dependent relaxation time listed in Table 2 could be well fitted by the Williams–Landel–Ferry (WLF) equation according to previous works:^{25,27,28,30,31}

$$\log \frac{\tau}{\tau_s} = \frac{-C_1 \times (T - T_s)}{C_2 + T - T_s} \quad (2)$$

Taking $C_1 = 8.86$ K and $C_2 = 101.6$ K, the WLF equation can be written as^{25,27,28,30,31}

$$\tau = \tau_s \times \exp\left(\frac{-2.303 \times 8.86 \times (T - T_s)}{101.6 + T - T_s}\right) \quad (3)$$

As shown in Figure 3a, the relaxation times of both samples obey the time–temperature superposition principle and can be described by the WLF equation well. The τ_s of PEI-13Sep2 obtained from simulation showed a much higher value than that of PEI-13, which means that the addition of fillers enhanced the viscoelasticity of the phase separation clearly.

The results of OM and TRLS can also be verified by SEM micrographs (Figure 3c and d). Both OM and SEM show the same characteristic length scale. It is quite clear that the final phase structures of samples with sepiolite were much more refined and sophisticated compared to that of sample without fillers.

Furthermore, by changing the surface affinity of meso-filters, a similar effect of refining phase structure is also observed from the addition of meso-filters. As previous work reported, meso-filters prefer to disperse in the slow dynamic phase (and phase boundary) due to the low mobility of meso-filters, asymmetric stress division, and restriction from the entanglements of fillers with long molecular chains.²⁵ The fillers added enlarge the dynamic asymmetry between the fast and slow components by dispersing in and hardening the slow component-rich phase. The entanglements of PEI chains on the meso-filler surface led

to the growth in elastic and viscous moduli of the PEI-rich phase, which in turn slowed down the disentanglement of polymer chains and resulted in enlargements of the relaxation time of the network.

3.2. Effect of meso-Fillers in Blends at Off-Critical Composition.

As meso-filters showed significant enhanced viscoelastic effect on the SD phase separation and final morphology, one would anticipate that these fillers may also influence the NG phase separation due to the same reason of chain entanglement.

To verify this point, we have studied a series of PEI–epoxy systems with low PEI concentration, such as 1, 3, and 5 wt % PEI, which were all of off-critical compositions. Systems both with and without meso-filters were studied. Taking PEI-5% and PEI-5%Sep2 as examples, the blends do not follow the SD mechanism, as TRLS showed little change of light-scattering profiles (only changes in light intensity) during the curing process, which always suggested that the system may follow the NG mechanism.²⁸

Figure 4 showed the morphology of the PEI-5 system with and without meso-filters. Like previous works of low volume fraction thermoplastic modified thermosetting resins, the PEI-5 system showed PEI dispersed phase structures (Figure 4a) with PEI domain size ca. 0.5–1.5 μm , which were formed via the NG process as “moving droplet phase” during the PIVPS.

Quite interestingly, with addition of meso-filters, except the little cracks on the surface, the PEI particles seem to disappear completely in the PEI-5Sep2 systems (Figure 4b), while only white dots of submicrometer size can be found dispersing in the epoxy matrix, which was a little similar to the epoxy resins blended with sepiolite (Ep-Sep2 in Figure 4c). With TEM, one can also find that there were almost only sepiolite particles being observed in the blends (Figure 4d), although the sepiolite seemed to be wrapped with PEI and formed some clusters.

This kind of disappearance of the droplet phase can be observed in other meso-filler added dynamic asymmetric systems with NG progress. In fact, we have tried other thermoplastics with low volume fraction, like poly(methyl methacrylate), poly(ethersulfone), polystyrene, and poly(acrylonitrile-butadiene-styrene) modified epoxy resins with either sepiolite or fumed silica fillers, and even high molecular weight rubber (polyepichlorohydrin) modified thermosetting resin with meso-filters showed a similar phenomenon.

Therefore, on the basis of the above experimental results, one can postulate the following two possibilities: (1) the addition of meso-filters hindered the phase separation caused by either thermodynamic or kinetic reasons and thus the blends formed a homogeneous structure; (2) meso-filters served as nucleation centers in the NG process, and the slow dynamic phase enwrapped on the meso-filters due to chain entanglement from the “enhanced viscoelastic effect”.

To verify these probabilities, other experimental methods, like rheological and thermo-mechanical studies, were applied to clarify the fundamental effect of meso-filters in the phase separation of off-critical composition systems.

3.3. Rheological Behavior during Phase Separation.

During the phase separation study of thermosetting resins, numerous studies have demonstrated the close relationship between rheological behavior and the phase separation process.^{28,35–41} The formation or breaking down of thermoplastic (high viscosity, slow dynamic phase) matrix always accompanies distinct fluctuations in both viscosity and

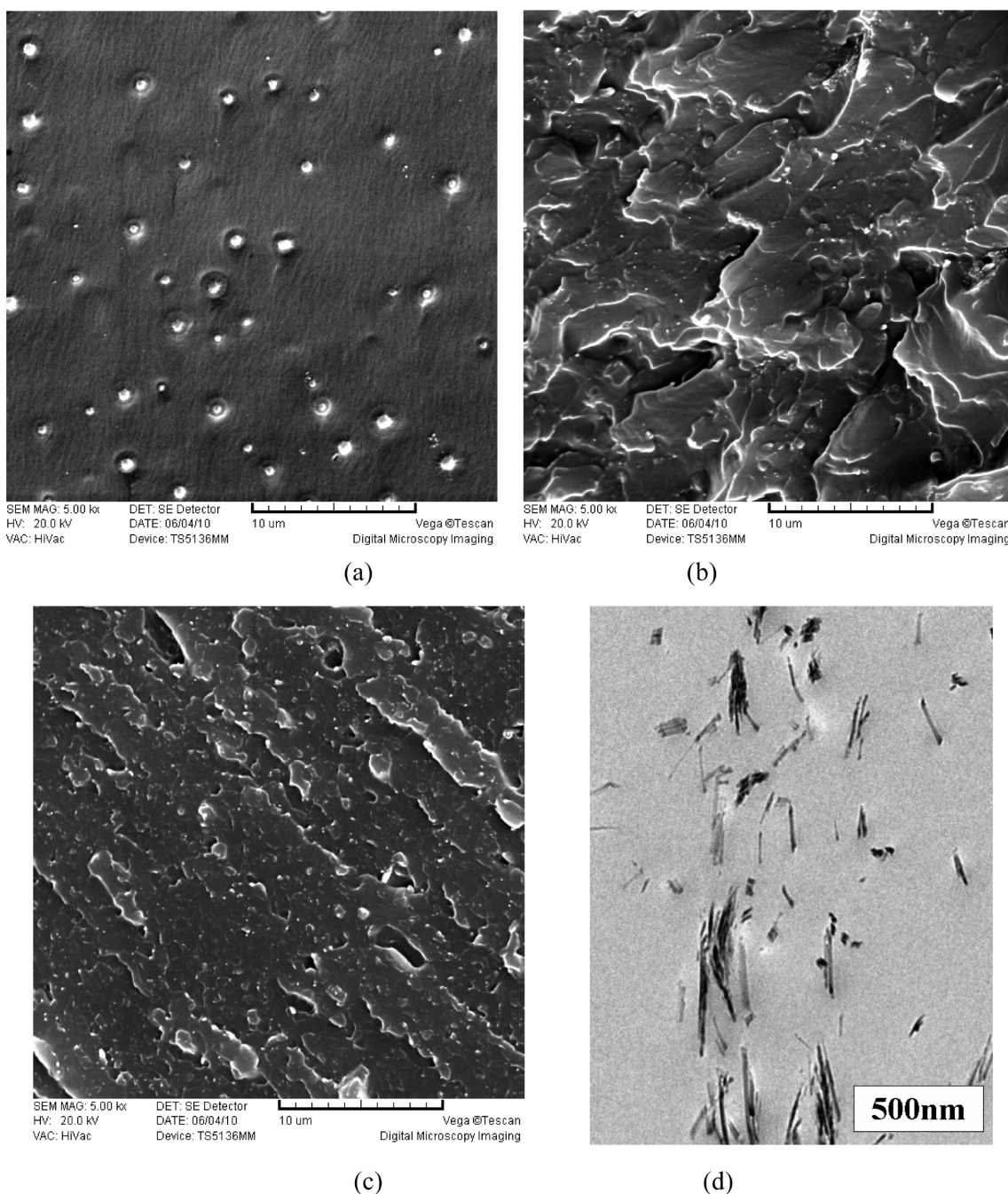


Figure 4. Phase structure of PEI-5, PEI-5Sep2, and Ep-Sep2 cured at 150 °C: (a) morphology of PEI-5 observed by SEM; (b) morphology of PEI-5Sep2 observed by SEM; (c) morphology of Ep-Sep2 observed by SEM; (d) morphology of PEI-5Sep2 observed by TEM.

modulus, which can be employed to identify the taking place of phase separation or structural transition.

Figure 5a and b showed the rheological behavior of neat epoxy and Ep-Sep2 systems cured at 150 °C; as one can see, the addition of sepiolite showed a minor effect on the viscosity and modulus evolution. The initial viscosity and modulus increased, while the curing rate decreased and gelation time prolonged slightly with the addition of sepiolite.

However, the rheological behavior of PEI-13 and PEI-13Sep2 clearly indicated the phase separation and structural transitions (in Figure 5c and d). In Figure 5c, the complex viscosities η^* of two blends were plotted at the same curing temperature. The addition of meso-fillers increased the initial viscosity; at about 100 s, the complex viscosity of both samples increased sharply

due to the phase separation and formation of bicontinuous structure.^{28,35–41} As we know from viscoelastic phase separation systems of thermoplastic-modified thermosets, the phase structures at the initial stage of phase separation are always phase inverted or thermoplastic as the continuous matrix;^{28,42} therefore, the thermoplastic-rich phase showed an increase in viscosity compared to that of the homogeneous mixture. However, the PEI-13 system, which had a sea-island phase structure, showed a quick drop in viscosity at about 300 s just after the initial increase. This subsequent decrease in viscosity was attributed to the breaking up of thermoplastic matrix structure as the network reverted back to a predominantly epoxy continuous matrix.^{28,36,37,41,42} This kind of viscosity fluctuation was not observed in the PEI-13Sep2

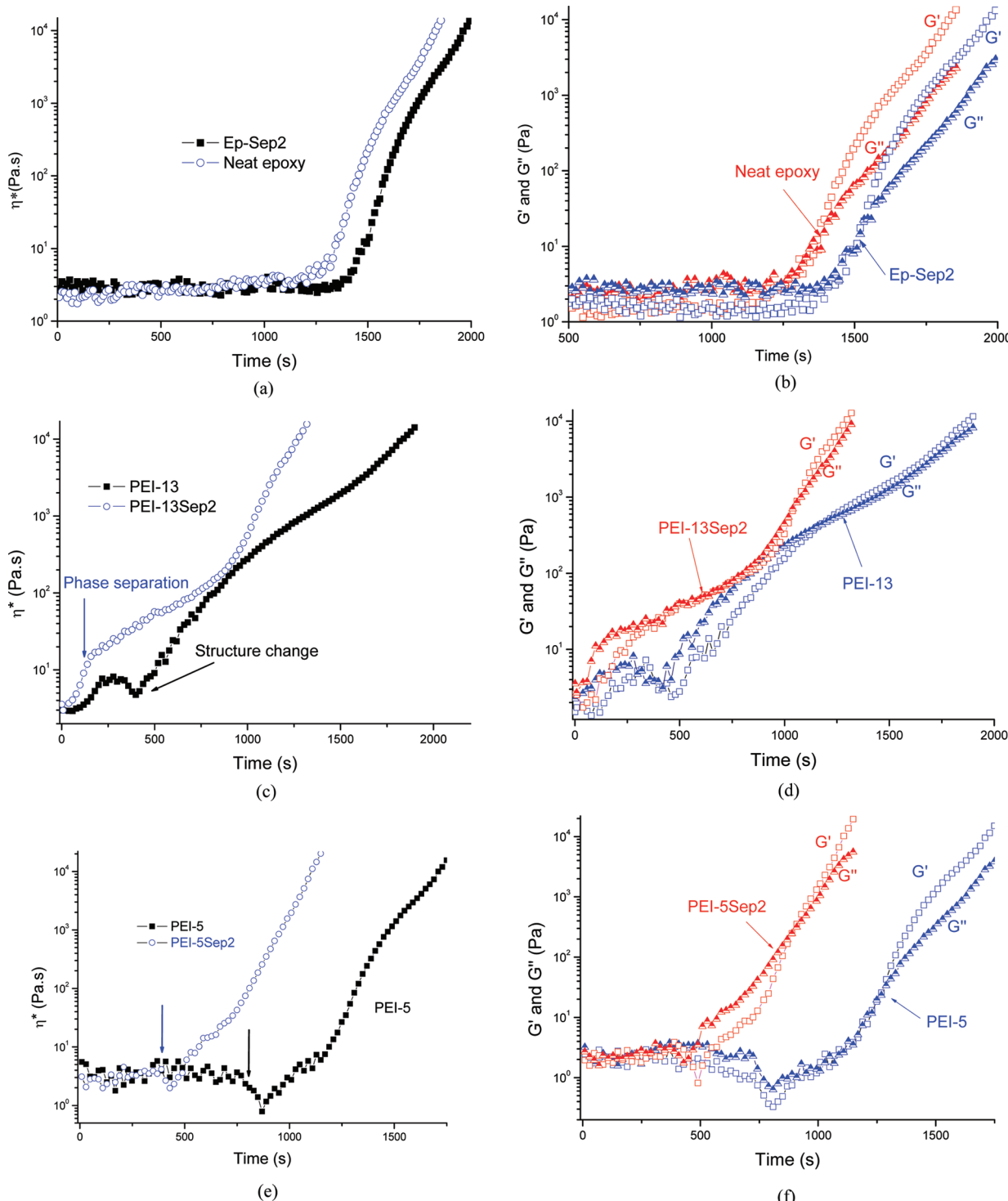


Figure 5. Rheological behavior of the PEI modified systems with and without meso-filters upon curing at 150 °C: (a) complex viscosity of neat epoxy and Ep-Sep2 systems and (b) storage and loss modulus of neat epoxy and Ep-Sep2 systems; (c) complex viscosity of PEI-13 and PEI-13Sep2 systems; (d) storage and loss modulus of PEI-13 and PEI-13Sep2 systems; (e) complex viscosity of PEI-5 and PEI-5Sep2 systems; (f) storage and loss modulus of PEI-5 and PEI-5Sep2 systems.

system as the addition of meso-filters pins down the phase separation process and keeps the bicontinuous structure. The storage and loss modulus corresponded well with the complex viscosity change of the two systems, respectively (in Figure 5d).

Although the two systems have an almost identical relationship between isothermal curing conversion versus time as studied by DSC (the addition of sepiolite slows

down curing rate slightly; the plot is not shown here), the viscosity and modulus change showed large differences: the meso-filler added system has a higher value and slightly earlier gelation time (crossover time of G' and G'') compared to the nonfiller system mainly due to the phase structure differences.

Interestingly, the PEI-5 systems showed large differences to PEI-5Sep2 systems (Figure 5e,f). In Figure 5e, PEI-5Sep2

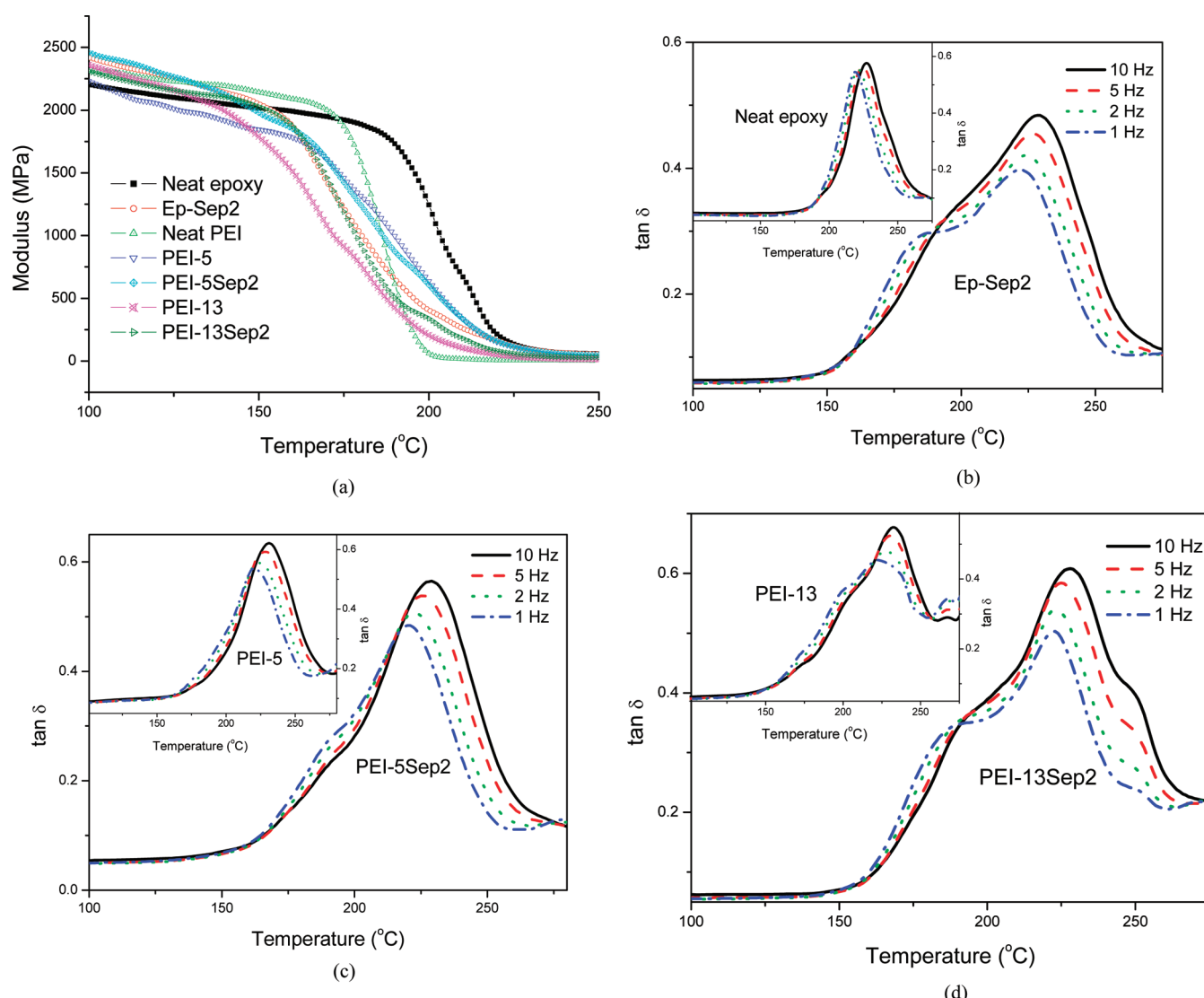


Figure 6. Dynamic mechanical study of the cured systems of epoxy resin and modified systems: (a) storage modulus versus temperature; (b) multifrequency dependency of $\tan \delta$ of neat epoxy and Ep-Sep2; (c) multifrequency dependency of $\tan \delta$ of PEI-5 and PEI-5Sep2; (d) multifrequency dependency of $\tan \delta$ of PEI-13 and PEI-13Sep2.

Showed an abrupt dropping of complex viscosity at about 480 s, while PEI-5 took place at ca. 800 s (marked by arrows in Figure 5f), which definitely indicated the NG phase separation process of the two systems as the nucleation of PEI-rich particles drops down the viscosity of the mixtures obviously (compared with Figure 5a and b of epoxy systems without meso-filters). Furthermore, the PEI-5Sep2 showed a much higher viscosity than that of the PEI-5 system once phase separation was taking place, and the moduli had a similar tendency as viscosity change in Figure 5f.

As the meso-filters are much larger in size than the polymer chains, the addition of sepiolite shows a minor effect on the phase diagram, which has been studied in our previous work by blending with a slow curing epoxy-anhydride system.²⁵ In other words, this dramatic change of phase separation process comes from kinetic factors rather than thermodynamic changes, emulsifying effect, or specific interactions.

From both morphology observation and rheological study of meso-filters added systems of off-critical concentration, it seems that the meso-filters most likely perform as nucleation centers for PEI-rich during the NG process. As a common knowledge,

the addition of nucleation agent favors the precipitation of polymers during phase separation, and thus, the initial phase separation time of PEI-13Sep2 was much smaller than that of PEI-13. Once phase separation taking place, the slow dynamic phase enwrapped on the meso-filler surface (or chain entangled with meso-filters) to form elastic gel particles of meso-size.^{8,43} Combined with the meso-filters and phase separation, a percolation network could therefore be generated,⁴⁴ which increases the viscosity of the system sharply and induces earlier gelation as compared with that of a nonfiller system as PEI-5.

Unlike SD phase separation, the NG process resulted in elastic droplets of high concentration slow dynamic component; the addition and chain entanglement of meso-filters further increase elasticity of the dispersed droplet phase. Then, we can therefore expect that the chain mobility of the slow dynamic phase (droplets) would be much more difficult than that of neat thermoplastic, and the chain entanglement with meso-filters would enhance this tendency conspicuously as both morphology and rheology show remarkable differences.

3.4. Viscoelastic Behavior of Phase Separated Blends.

To confirm the above discussions on the enhanced viscoelastic

effect of meso-filters on the PIVPS, we studied the viscoelastic behavior of the fully cured PEI modifying epoxy systems with and without meso-filler sepiolite by DMA. In Figure 6a, the storage moduli of all the samples are illustrated. Neat epoxy showed the highest temperature value for the dropping down of modulus, while PEI has a lower temperature value than that of epoxy. The addition of PEI also decreases the initial dropping of the modulus. As commercial DMA instruments have a relatively low accuracy in measuring forces and/or strains, the moduli of all the samples are relative comparable; it can be seen that the addition of meso-filters increased the modulus of modified systems to some extent.

In contrast, DMA gives relatively accurate values of the damping factor $\tan \delta$, so that dissipation spectra $\tan \delta = f(\omega; T)$ are very useful analytical tools. To give a clear description of the T_g change with the addition of PEI and meso-filters, the multifrequency $\tan \delta$ versus temperature of the samples are plotted in Figure 6b, c, and d. Compared with neat epoxy, Ep-Sep2 with meso-filters showed another new peak of $\tan \delta$ at lower temperature, which can be easily identified by splitting the peaks into two isolated peaks. Similarly, all the samples with PEI and meso-filters showed two peaks and can also be isolated by splitting peaks.

Table 3 showed the glass transition temperatures of the entire samples tested at the frequency of 1 Hz from Figure 6.

Table 3. Glass Transition Temperature, Apparent Activation Energy, and Impact Strength of the Samples

	Tg ^a (°C)	Tg ^a (°C)	ΔE ^b (kJ/mol)	ΔE ^b (kJ/mol)	impact strength ^c (kJ/m ²)
neat epoxy	219.2		589		9.2 ± 0.9
neat PEI	200.8		727		
Ep-Sep2	186.5	223.2	320	505	9.7 ± 0.8
PEI-5	191.6	222.3	1125	557	7.5 ± 0.7
PEI-SSep2	191.9	221.9	3958	707	14.8 ± 1.1
PEI-13	200.9	225.6	612	585	12.4 ± 1.1
PEI-13Sep2	189.3	222.3	487	699	12.9 ± 1.0

^aGlass transition temperature obtained from DMA of $\tan \delta$ at 1 Hz.

^bApparent activation energy calculated on the basis of eq 4. ^cIzod impact strength of unnotched cantilever beam tested according to ISO 180-2000 at room temperature.

All the PEI modified systems show two separated glass transition temperatures corresponding to either PEI-rich or epoxy-rich phases, which were comparable to the values of neat epoxy and PEI.^{28,52}

As the glass transition process corresponds to the relaxation process of polymer chain segments, the apparent activation energy of the relaxation process is determined by the peak temperature T_p from the following equation:⁵³

$$\omega\tau = 2\pi f\tau_0 e^{E_a/k_B T_p} = 1 \quad (4)$$

where ω is the angular frequency, τ relaxation time, f the frequency, E_a the apparent activation energy for the relaxation process, and k_B the Boltzmann constant. Thus, the natural logarithm of frequency is plotted as a function of $1/T$, and the fitted straight line was determined by the least-squares method. We see a good linear fit between $\ln f$ and $1/T$ for the peaks in Figure 7a and b (Ep-Sep2 and PEI-SSep2 are shown as

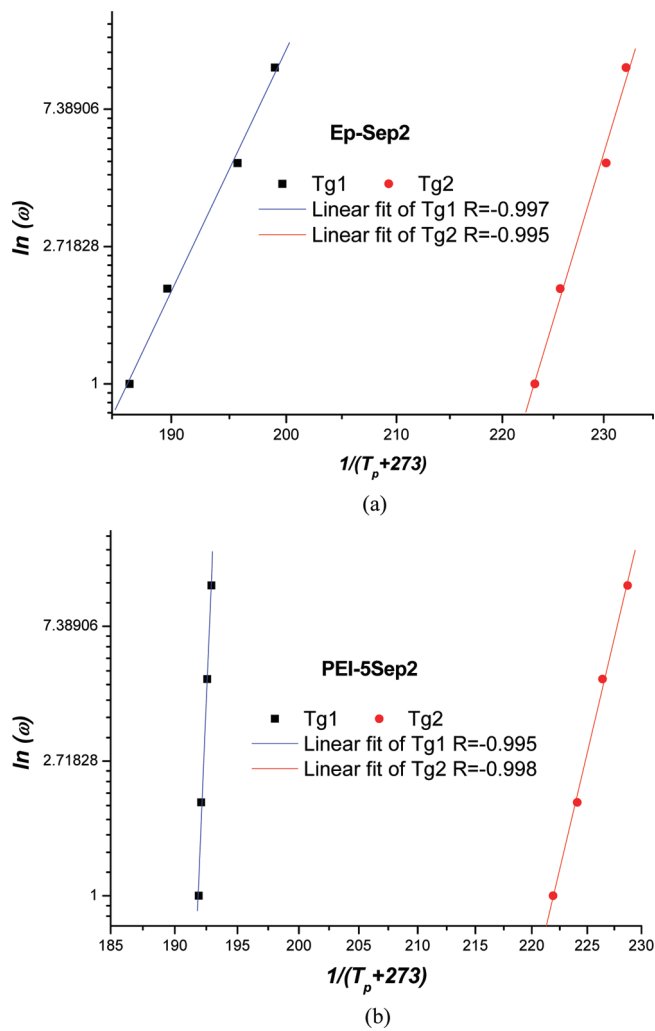


Figure 7. The plots of $\ln(\text{frequency})$ versus $1/(T_g)$ for epoxy with sepiolite and PEI: (a) Ep-Sep2; (b) PEI-SSep2.

examples). From the slope of the fitted line, the apparent activation energy can be determined and listed in Table 3.

The E_a values of neat epoxy and PEI are 589 and 727 kJ/mol, respectively. As numerous studies have demonstrated, the addition of nanofillers always decreases the glass transition temperature of epoxy resins perhaps due to the extra free volume at the resin–filler interface or lower cross-link density.^{45–47} Nevertheless, one can find that the meso-filters deduced the epoxy networks into two parts: one part nearly fully cured with chain mobility close to neat epoxy ($E_a = 505$ kJ/mol) while another part with much higher chain mobility at lower temperature range ($E_a = 320$ kJ/mol).

For PEI modified systems without meso-filters, the T_g of the epoxy-rich phase was quite close to that of neat epoxy. However, the T_g of PEI-rich showed two tendencies: depressed in PEI-13 while increased in PEI-5. Considering the different phase separation mechanism of the two systems via SD and NG, one can deduce the depression of T_g in PEI-13 coming from the SD process of slow concentration fluctuation,⁴⁸ which resulted in an incompletely phase separated PEI-rich phase with a considerably high amount of epoxy molecules (low E_a). The NG process of PEI-5 results in a relative higher concentration of nucleated PEI particles of elastic stressing,⁸ which further

increase the difficulty of PEI chain mobility, and thus cause PEI-rich of high E_a .

Apparently, the addition of meso-filters enhanced this trend of E_a variation. For PEI-13Sep2, due to the enhanced viscoelastic effect of meso-filters, the phase separation is pinned down at an earlier stage; i.e., the PEI-rich phase composes higher concentration of epoxy, and thus possesses lower E_a value than that of PEI-13. On the contrary, the epoxy-rich phase encompasses a higher concentration of PEI, and therefore shows higher E_a than that of PEI-13 and neat epoxy resin.

For PEI-5Sep2 during NG process, the nucleation of PEI on the meso-filters with high elastic stressing may deduce oriented PEI chains along the meso-filter surface, which thereby exacerbates the low mobility of PEI chains and conduced to the sharp increase of E_a . At the same time, the well dispersion of PEI-enwrapped meso-filters in epoxy network may further restrict the chain mobility of epoxy resins, and hence increase the E_a of the epoxy-rich phase.

The toughness study of samples can also give a relative comparison of phase structure change due to the addition of meso-filters. The unnotched izod impact strengths provide sufficient evidence of morphology changes. The addition of sepiolite in epoxy (Ep-Sep2) gives a limited increase of impact strength relative to neat epoxy resin, while the low concentration of PEI seems to deteriorate the toughness of modified systems to some extent. Only with high concentration of PEI as in PEI-13 can the toughness be increased obviously due to the formation of PEI continuous structure.^{49–51} After sepiolite is added to the PEI-13 system, the bicontinuous phase structure is maintained and a more refined continuous network is formed due to the enhanced viscoelastic effect of meso-filters; therefore, one can see that the adding of sepiolite evidently improves the toughness of the PEI-13Sep2 relative to epoxy resin modified with either PEI or sepiolite alone.

However, PEI-5Sep2 shows the highest impact strength value, which is almost twice of PEI-5's toughness and about 50% higher than that of neat epoxy resin. This kind of great improvement in toughness is evidently attributed to the specific phase structure of thermoplastic enwrapped sepiolite via NG mechanism. In fact, we have tested various systems of low concentration thermoplastics (off-critical concentration slow dynamic component) modified epoxy resins combined with meso-filters; for example, 2 wt % of poly(ethersulfone) and poly(acrylonitrile-butadiene-styrene) modified epoxy resins with 1% sepiolite show much higher impact strength compared with higher concentration thermoplastic modified systems. In other words, the “enhanced viscoelastic effect” of meso-filters in PIVPS of near- and off-critical composition is not only rather interesting in terms of theoretical study but also very important to industrial applications.

4. CONCLUSIONS

The “enhanced viscoelastic effect” of mesoscopic fillers is universal in different phase-separation systems as long as dynamic asymmetry exists. For both spinodal decomposition and nucleation and growth mechanisms, the slow part (viscous component) is preferential to chain entangle with mesoscopic fillers (or on the surface), and thus form a refined network or enwrapped mesoscopic fillers depending on the location of mixture composition in the phase diagram. In the nucleation and growth phase separation process, mesoscopic fillers serve as the nuclear center and also being highly chain entangled by the

slow part to form enwrapped particles with very low mobility of polymer chains, which are quite beneficial to the toughness of modified systems. The rheological behavior evolution and thermo-mechanical properties of the cured blends were consistent with the morphology variation due to the addition of mesoscopic fillers.

■ AUTHOR INFORMATION

Corresponding Author

*Phone: +86 21 6564 2865. Fax: +86 21 6564 0293. E-mail: yfyu@fudan.edu.cn.

Notes

The authors declare no competing financial interest.

■ ACKNOWLEDGMENTS

We acknowledge support from the National Nature Science Foundation of China (grants 20704008 and 20974027) and the Scientific Research Foundation for the Returned Overseas Chinese Scholars, State Education Ministry.

■ REFERENCES

- (1) Iwashita, Y.; Tanaka, H. *Nat. Mater.* **2006**, *5*, 147–152.
- (2) Kietzke, T.; Neher, D.; Landfester, K.; Montenegro, R.; Guntner, R.; Scherf, U. *Nat. Mater.* **2003**, *2*, 408–412.
- (3) Hohenberg, P. C.; Halperin, B. I. *Rev. Mod. Phys.* **1977**, *49*, 435–479.
- (4) Cahn, J. W. *J. Chem. Phys.* **1965**, *42*, 93–99.
- (5) Lifshitz, I. M.; Slyozov, V. J. *Phys. Chem. Solids* **1961**, *19*, 35–50.
- (6) Wagner, C. Z. *Elektrochem.* **1961**, *65*, 581–591.
- (7) Furukawa, H. *Adv. Phys.* **1985**, *34*, 703–750.
- (8) Tanaka, H. *J. Phys.: Condens. Matter* **2000**, *12*, R207–R264.
- (9) Tanaka, H. *Phys. Rev. Lett.* **1993**, *71*, 3158–3161.
- (10) Tanaka, H. *J. Chem. Phys.* **1994**, *100*, 5323–5337.
- (11) Tanaka, H.; Lovinger, A. J.; Davis, D. D. *Phys. Rev. Lett.* **1994**, *72*, 2581–2584.
- (12) He, L. L.; Zhang, L. X.; Liang, H. *J. Phys. Chem. B* **2008**, *112*, 4194–4203.
- (13) Li, Y.; Shimizu, H. *Macromolecules* **2008**, *41*, 5339–5344.
- (14) Bockstaller, M. R.; Thomas, E. L. *Phys. Rev. Lett.* **2004**, *93*, 166106.
- (15) Kietzke, T.; Neher, D.; Kumke, M.; Ghazy, O.; Ziener, U.; Landfester, K. *Small* **2007**, *3*, 1041–1048.
- (16) Hore, M. J. A.; Laradji, M. *J. Chem. Phys.* **2008**, *128*, 054901.
- (17) Tian, P.; Smith, G. D. *J. Chem. Phys.* **2006**, *124*, 184701.
- (18) Ginzburg, V. V. *Macromolecules* **2005**, *38*, 2362–2367.
- (19) Schultz, A. J.; Hall, C. K.; Genzer, J. *Macromolecules* **2005**, *38*, 3007–3016.
- (20) Laradji, M.; Hore, M. J. A. *J. Chem. Phys.* **2004**, *121*, 10641–10647.
- (21) Si, M.; Araki, T.; Ade, H.; Kilcoyne, A. L. D.; Fisher, R.; Sokolov, J. C.; Rafailovich, M. H. *Macromolecules* **2006**, *39*, 4793–4801.
- (22) Yurekli, K.; Karim, A.; Amis, E. J.; Krishnamoorti, R. *Macromolecules* **2003**, *36*, 7256–7267.
- (23) Ray, S. S.; Bousmina, M. *Macromol. Rapid Commun.* **2005**, *26*, 1639–1646.
- (24) Vo, L. T.; Giannelis, E. P. *Macromolecules* **2007**, *40*, 8271–8276.
- (25) Zhong, X.; Liu, Y.; Su, H.; Zhan, G.; Yu, Y.; Gan, W. *Soft Matter* **2011**, *7*, 3642–3650.
- (26) Wheeler, P. A.; Wang, J. Z.; Baker, J.; Mathias, L. J. *J. Chem. Mater.* **2005**, *17*, 3012–3018.
- (27) Gan, W. J.; Yu, Y. F.; Wang, M. H.; Tao, Q. S.; Li, S. J. *Macromolecules* **2003**, *36*, 7746–7751.
- (28) Yu, Y. F.; Wang, M. H.; Gan, W. J.; Tao, Q. S.; Li, S. J. *J. Phys. Chem. B* **2004**, *108*, 6208–6215.

- (29) Jose, J.; Joseph, K.; Pionteck, J.; Thomas, S. *J. Phys. Chem. B* **2008**, *112*, 14793–14803.
- (30) Jyotishkumar, P.; Koetz, J.; Tiersch, B.; Strehmel, V.; Ozdilek, C.; Moldenaers, P.; Hassler, R.; Thomas, S. *J. Phys. Chem. B* **2009**, *113*, 5418–5430.
- (31) Jyotishkumar, P.; Ozdilek, C.; Moldenaers, P.; Sinturel, C.; Janke, A.; Pionteck, J.; Thomas, S. *J. Phys. Chem. B* **2010**, *114*, 13271–13281.
- (32) Goossens, S.; Goderis, B.; Groeninckx, G. *Macromolecules* **2006**, *39*, 2953–2963.
- (33) Zhang, Y.; Shi, W. C.; Chen, F. H.; Han, C. C. *Macromolecules* **2011**, *44*, 7465–7472.
- (34) Nakanishi, H.; Satoh, M.; Norisuye, T.; Tran-Cong-Miyata, Q. *Macromolecules* **2006**, *39*, 9456–9466.
- (35) Bonnet, A.; Camberlin, Y.; Pascault, J. P.; Sautereau, H. *Macromol. Symp.* **2000**, *149*, 145–150.
- (36) Kim, H.; Char, K. *Ind. Eng. Chem. Res.* **2000**, *39*, 955–959.
- (37) Yu, Y. F.; Zhang, Z. C.; Gan, W. J.; Wang, M. H.; Li, S. *J. Ind. Eng. Chem. Res.* **2003**, *42*, 3250–3256.
- (38) Tercjak, A.; Remiro, P. M.; Mondragon, I. *Polym. Eng. Sci.* **2005**, *45*, 303–313.
- (39) Gan, W. J.; Zhan, G. Z.; Wang, M. G.; Yu, Y. F.; Xu, Y. Z.; Li, S. *J. Colloid Polym. Sci.* **2007**, *285*, 1727–1731.
- (40) Tribut, L.; Fenouillot, F.; Carrot, C.; Pascault, J. P. *Polymer* **2007**, *48*, 6639–6647.
- (41) Bonnet, A.; Pascault, J. P.; Sautereau, H.; Camberlin, Y. *Macromolecules* **1999**, *32*, 8524–8530.
- (42) Yu, Y. F.; Wang, M. H.; Foix, D.; Li, S. *J. Ind. Eng. Chem. Res.* **2008**, *47*, 9361–9369.
- (43) Tanaka, H. *Phys. Rev. Lett.* **1996**, *76*, 787–790.
- (44) Peng, G. W.; Qiu, F.; Ginzburg, V. V.; Jasnow, D.; Balazs, A. C. *Science* **2000**, *288*, 1802–1804.
- (45) Sun, Y. Y.; Zhang, Z. Q.; Moon, K. S.; Wong, C. P. *J. Polym. Sci., Part B: Polym. Phys.* **2004**, *42*, 3849–3858.
- (46) Putz, K. W.; Palmeri, M. J.; Cohn, R. B.; Andrews, R.; Brinson, L. C. *Macromolecules* **2008**, *41*, 6752–6756.
- (47) Ash, B. J.; Schadler, L. S.; Siegel, R. W. *Mater. Lett.* **2002**, *55*, 83–87.
- (48) Girard-Reydet, E.; Sautereau, H.; Pascault, J. P.; Keates, P.; Navard, P.; Thollet, G.; Vigier, G. *Polymer* **1998**, *39*, 2269–2279.
- (49) Oyanguren, P. A.; Frontini, P. M.; Williams, R. J. J.; Vigier, G.; Pascault, J. P. *Polymer* **1996**, *37*, 3087–3092.
- (50) Pethrick, R. A.; Hollins, E. A.; McEwan, I.; MacKinnon, A. J.; Hayward, D.; Cannon, L. A.; Jenkins, S. D.; McGrail, P. T. *Macromolecules* **1996**, *29*, 5208–5214.
- (51) DiPasquale, G.; Motta, O.; Recca, A.; Carter, J. T.; McGrail, P. T.; Acierno, D. *Polymer* **1997**, *38*, 4345–4348.
- (52) Paul, D. R.; Bucknall, C. C. *Polymer blends; Formulation*, Vol. 1; John Wiley & Sons: New York, 2000.
- (53) Garwe, F.; SchoInhals, A.; Lockwenz, H.; Beiner, M.; Schrolter, K.; Donth, E. *Macromolecules* **1996**, *29*, 247–253.